er, even small changes in STREX expression producing subtle changes in chromaffin cell excitability could have pronounced effects on the secretion of catecholamines and other products (including corticosteroids through reciprocal interactions with the adrenal cortex) (*21*), with potentially far-reaching consequences in humans. Among the functions likely to be affected to some extent are cardiovascular, digestive, metabolic, immune, and mental functions (*22*). Changes in chromaffin BK channels in response to hormonally communicated stress represent another dimension of stress-related plasticity in adrenal tissue.

Tissue-specific and developmental regulation of alternative splicing is well established for many genes, with factors and mechanisms being worked out. Reports of dynamic regulation of splicing patterns in adult tissues are rare (*23*). Exons in complex modular proteins such as ion channels often comprise discrete functional units, and dynamic hormonal control of exon selection provides a unique dimension for regulating the often critical functional nuances of the whole protein.

REFERENCES AND NOTES

1. M. E. Ross *et al.*, *J. Neurosci.* **10**, 520 (1990); S. N. Ebert *et al.*, *J. Biol. Chem.* **269**, 20885 (1994).
2. E. S. Levitan, K. M. Hershman, T. G. Sherman, K. Takimoto, *Neuropharmacology* **35**, 1001 (1996); K. Takimoto and E. S. Levitan, *Circ. Res.* **75**, 1 (1994); K. Takimoto, A. F. Fomina, R. Gealy, J. S. Trimmer, E. S. Levitan, *Neuron* **11**, 359 (1993); B. Attardi, K. Takimoto, R. Gealy, C. Severns, E. S. Levitan, *Receptors Channels* **1**, 287 (1993).
3. C. R. Solaro, M. Prakriya, J. P. Ding, C. J. Lingle, *J. Neurosci.* **15**, 6110 (1995).
4. C. J. Lingle, C. R. Solaro, M. Prakriya, J. P. Ding, *Ion Channels* **4**, 261 (1996).
5. A. Butler, S. Tsunoda, D. P. McCobb, A. Wei, L. Salkoff, *Science* **261**, 221 (1993); J. Tseng-Crank *et al.*, *Neuron* **13**, 1315 (1994).
6. J. P. Adelman *et al.*, *Neuron* **9**, 209 (1992); N. S. Atkinson, G. A. Robertson, B. Ganetzky, *Science* **253**, 551 (1991).
7. M. K. Stachowiak, R. J. Rigual, P. H. K. Lee, O. H. Viveros, J. S. Hong, *Mol. Brain Res.* **3**, 275 (1988); E. Viskupic *et al.*, *J. Neurochem.* **63**, 808 (1994).
8. J. Xie, P. Lappas, W. Yao, E. Carpenter-Hyland, D. P. McCobb, *Soc. Neurosci. Abstr.* **22**, 402 (1996). For calibrated RT-PCR, different amounts of calibrator template cRNA {constructed as per S. Diviacco *et al.* [*Gene* **122**, 313 (1992)]} were added to identical 12.5-ng samples of tissue RNA. Relative PCR product band intensity was measured with BIT Image 1.55 (Digital Imagers, Elburn, IL). We measured the native template by extrapolating to the calibrator template amount yielding equivalent product bands, with corrections for length effects on amplification efficiency and band intensity.
9. Sprague-Dawley rats (Charles River) were hypophysectomized with the parapharyngeal approach to the occipitosphenoid suture. After trephination, the hypophysis was removed by aspiration. Hypophysectomized rats received 5% sucrose water. Marked reductions in adrenal cortical volume and rat body weight at death, compared with age- and sex-matched rats, indicated successful hypophysectomy.
10. M. Saito, C. Nelson, L. Salkoff, C. J. Lingle, *J. Biol. Chem.* **272**, 11710 (1997).
11. J. Ferrer, J. Wasson, L. Salkoff, M. A. Permutt, *Diabetologia* **39**, 891 (1996).
12. J. Xie and D. P. McCobb, *Soc. Neurosci. Abstr.* **23**, 309 (1997). The ratio of STREX to ZERO isoform varied only slightly more between left and right glands from a single animal (N = 14 pairs) than between replicate measures on a single mRNA sample, supporting the quantitative reproducibility of the approach. Total RNA was extracted from dissected adrenal medullas, and 200 ng was used in a 10-μl RT reaction with 200 U of Superscriptase II and oligo$(dT)_{22}$ (Gibco BRL). One microliter of RT product was used in a 25-μl PCR for 30 cycles at 94°C, 30-s denaturation; 55°C, 30-s annealing; and 72°C, 30-s extension. Five microliters of product was run on a 2% agarose gel stained with ethidium bromide.
13. ACTH was in gel form (Rhone Poulenc Rorer Pharmaceutical, Collegeville, PA).
14. R. E. Coupland, *The Natural History of the Chromaffin Cell* (Longmans, London, 1965); R. J. Wurtman and J. Axelrod, *J. Biol. Chem.* **241**, 2301 (1966).
15. IMMUCHEM Double Antibody Corticosterone RIA kit (ICN, Irvine, CA) was used by the veterinary diagnostic lab at Cornell University. Corticosterone was extracted from ground adrenals with 0.5 ml of ethyl acetate at room temperature and spun at 11,000 rpm for 5 min, and the upper phase was saved, vacuum dried, and resuspended in 400 μl of resuspension buffer with 5% ethanol.
16. Plasmid constructs for cRNA expression in *Xenopus* oocytes were devised by modification of a mouse Slo (mSlo) expression construct (*5*). Rat adrenal RT-PCR products corresponding to ZERO, STREX-1, and STREX-2 variants were made with primers rSlo3 and a downstream primer with an internal Xho I site (sequence: 5′-ACCGCTCGAGCTCTGGCGTGGCTCCTCCTG-3′) and cloned into unique Hind III and Xho I sites in the mSlo vector. Restriction analysis and sequencing were used to confirm constructs. mSlo differs from rSlo outside the rat insert at only 4 of 716 residues. Plasmids were linearized with Sal I and transcribed with Ambion T3 mMESSAGE kit.
17. Patch clamp solutions were potassium methanesulfonate based (pH 7.0). Free calcium concentrations were determined with a calcium-selective electrode (Orion, Beverly, MA). Procedure and solutions were as described by D. P. McCobb *et al.* [*Am. J. Physiol.* **269**, H767 (1995)]. A List EPC-7 patch clamp with ITC-16 data interface (Instrutech, NY) and Pulse software (HEKA, Lambrecht, Germany) were used for data acquisition.
18. D. P. McCobb, J. Xie, D. Baro, *Soc. Neurosci. Abstr.* **23**, 1477 (1997).
19. S. Ceccatelli, A. Dagerlind, M. Schalling, A.-C. Wikstorm, *Acta Physiol. Scand.* **137**, 559 (1989).
20. D. L. Wong, A. Lesage, B. Siddall, J. W. Funder, *FASEB J.* **6**, 3310 (1992); D. L. Wong, R. J. Hayashi, R. D. Ciaranello, *Brain Res.* **330**, 209 (1985).
21. G. G. Nussdorfer, *Pharmacol. Rev.* **48**, 495 (1996).
22. R. C. Lake and M. G. Ziegler, *The Catecholamines in Psychiatric and Neurologic Disorders* (Butterworth, Stoneham, MA, 1985).
23. J. E. Kraus, J. V. Nadler, J. O. McNamara, *Mol. Brain Res.* **41**, 97 (1996).

24. We thank R. Harris-Warrick, D. Baro, R. Knapp, A. Bass, and R. Hoy for helpful discussions. Supported by the American Heart Association.

25 November 1997; accepted 23 February 1998

Maternal Control of Embryogenesis by *MEDEA*, a *Polycomb* Group Gene in *Arabidopsis*

Ueli Grossniklaus,* Jean-Philippe Vielle-Calzada, Marilu A. Hoeppner, Wendy B. Gagliano†

The gametophytic maternal effect mutant *medea* (*mea*) shows aberrant growth regulation during embryogenesis in *Arabidopsis thaliana*. Embryos derived from *mea* eggs grow excessively and die during seed desiccation. Embryo lethality is independent of the paternal contribution and gene dosage. The *mea* phenotype is consistent with the parental conflict theory for the evolution of parent-of-origin–specific effects. *MEA* encodes a SET domain protein similar to *Enhancer of zeste*, a member of the *Polycomb* group. In animals, *Polycomb* group proteins ensure the stable inheritance of expression patterns through cell division and regulate the control of cell proliferation.

The plant life cycle alternates between diploid and haploid generations, sporophyte and gametophyte, as the haploid spores undergo several cell divisions before the gametes finally differentiate and fuse to produce the diploid zygote. We identified an *Arabidopsis thaliana* mutant, *medea* (*mea*), in which self-fertilization of the heterozygote produces 50% aborted seeds that collapse, accumulate anthocyanin, and do not germinate. This ratio of defective to normal seeds is consistent with a gametophytic control of the defect, because half the haploid gametophytes receive the mutant allele. Heterozygous embryos abort if the mutant allele is derived from the female (Fig. 1A), but develop normally if it is derived from the male (Fig. 1B and Table 1). Embryos derived from mutant eggs abort irrespective of the paternal contribution (*1*). Thus, the *mea* mutant displays maternal-effect embryo lethality (*2*). In flowering plants, embryo development is affected by both the female gametophyte (*3*) and the sporophytic tissue of the parent plant (*4*). The survival of the resultant embryo depends on the presence of a wild-type *MEA* allele in the genome of the female gametophyte.

Fertilization of the egg and central cell generates the diploid zygote and the triploid primary endosperm. Endosperm resulting

Cold Spring Harbor Laboratory, 1 Bungtown Road, Post Office Box 100, Cold Spring Harbor, NY 11724, USA.

*To whom correspondence should be addressed. E-mail: grossnik@cshl.org

†Present address: Graduate Program in Natural Resources, Ohio State University, Columbus, OH 43210–1085, USA.

from a cross between a wild-type male and a *mea-1* female carries two mutant *mea-1* alleles and one wild-type *MEA* allele. To determine whether seed abortion is caused by a mutation in a dosage-sensitive gene, we introduced additional wild-type *MEA* copies: In a cross between a *mea-1* heterozygous female and a wild-type tetraploid male, half of the fertilized seeds abort (Table 1) and the mutant *mea-1* allele is not recovered in the progeny (0/41). In control crosses, seeds rarely abort (Table 1), and paternal *mea-1* alleles are transmitted to half the offspring (66/124) suggesting that an additional paternal wild-type *MEA* allele is unable to rescue maternal-effect lethality. Thus, *mea* either affects a maternally produced cytoplasmic factor in the egg or central cell (or both), or disrupts an imprinted gene expressed from the maternal allele.

During early stages of embryogenesis the development of *mea-1* embryos is indistinguishable from wild-type siblings in cleared or sectioned specimens (5). Visible differences between wild-type and *mea-1* embryos began at the late globular stage (Fig. 1, C and D). Globular *mea-1* embryos show excess cell proliferation and enlarge radially symmetrical. When wild-type embryos reach the mid to late heart stage, sibling *mea-1* embryos are still globular and contain small vacuolated cells with curvilinear cell walls and sometimes irregular cell divisions in the ground tissue and procambium. Suspensor and hypophysis are normal, and cotyledons initiate synchronously as in the wild type. Thus, despite increased cell proliferation and occasional irregular cytokinesis, morphogenetic progression is normal. However, each stage is prolonged and includes more division cycles, and morphogenesis is delayed. As a consequence, giant heart stage *mea-1* embryos (Fig. 1, E and F) are present along with late torpedo or cotyledonary stage wild-type embryos. *mea-1* heart stage embryos have supernumerary cell layers (*mea-1*: 19.6 ± 1.1; wild type: 13.0 ± 0.9). When wild-type siblings are fully differentiated, most *mea-1* embryos have reached the late heart stage and are up to 10 times larger than normal. *mea* embryos degenerate during desiccation. These results suggest that *mea* controls cell proliferation during embryogenesis, allowing morphogenesis to progress normally, albeit slowly.

Endosperm development in *mea-1* seeds is indistinguishable from that of the wild type at early stages. When cellularization begins normally in wild-type seeds at the transition from the globular to the heart stage, no cellularization is observed in sibling *mea-1* seeds. Although nuclear divisions take place more slowly in *mea-1* endosperm, the distribution of endosperm nuclei is as in the wild type. Partial cellularization occurs at the micropyle when *mea-1* embryos reach the late heart stage in desiccating seeds, but because fewer nuclei have been generated, most of the central cell is devoid of nuclei. Thus, in *mea-1* seeds, the development of both fertilization products is delayed but morphogenesis proceeds normally, and it appears that the embryo shows increased cell proliferation at the expense of the endosperm.

To determine whether *mea-1* is a gain-of-function or loss-of-function mutation we introduced *mea-1* into a tetraploid back-

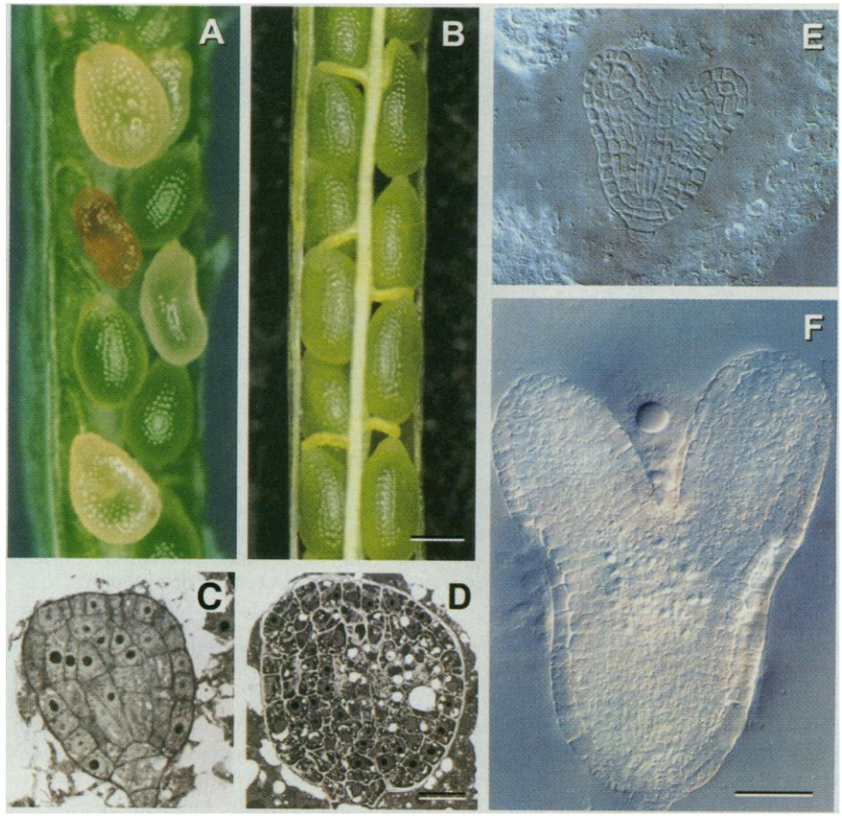

Fig. 1. Seed and embryo development in *mea* plants. (**A**) Silique resulting from a cross between *mea-1* (female) and a wild-type plant (male) of the Columbia (Col) ecotype. Seeds derived from *mea* female gametes turn white and collapse. (**B**) Silique resulting from a cross between Col (female) and *mea-1*(male). Histological analysis of embryos was conducted in heterozygous *mea-1* plants using semithin sections (C and D) and cleared seeds (E and F). (**C**) Late globular wild-type embryo. (**D**) Late globular *mea-1* embryo. (**E**) Late heart stage wild-type embryo. (**F**) Late heart stage *mea-1* embryo. Magnification: bar is 215 μm in (A) and (B); 12 μm in (C) and (D); and 40 μm in (E) and (F).

Table 1. Seed phenotype of reciprocal crosses between *mea* and diploid or tetraploid wild-type plants. Green or dry siliques resulting from self pollination or out-crosses to Columbia (Col) or a tetraploid plant were opened and the seeds classified as unfertilized ovules, normal, or aborted seeds. In crosses involving tetraploids, fertility is reduced because of a large fraction of unfertilized ovules (*29*). The relative increase in unfertilized ovules in the "Col × 4n" cross is due to longer siliques and a larger number of ovules per silique in Col plants (Col: 65.1 ± 6.4; *mea-1*: 39.7 ± 5.9; 4n: 43.6 ± 3.2). Pollen viability in tetraploids is reduced such that only ovules at the top of the silique get fertilized. The average number of seeds per silique initiating development is similar (Col: 17.9 ± 2.1; *mea-1*: 22.1 ± 5.9; 4n: 26.1 ± 4.4). The "normal" class includes brown, quite regularly shaped seeds that are smaller than those of the wild type and are common in crosses involving plants of different ploidy. They do not show the collapsed, black *mea* phenotype. *n* (seeds), number of seeds scored.

Female / Male	*mea-1* (selfed)	*mea-1* × Col	Col × *mea-1*	*mea-1* × 4n	Col × 4n	4n × *mea-1*	4n × Col	4n (selfed)
Unfertilized	12%	13%	11%	45%	72%	37%	40%	46%
Normal	42%	43%	88%	26%	27%	59%	54%	52%
Aborted	46%	44%	1%	29%	1%	4%	6%	2%
n (seeds)	1461	770	514	437	587	1155	696	1489

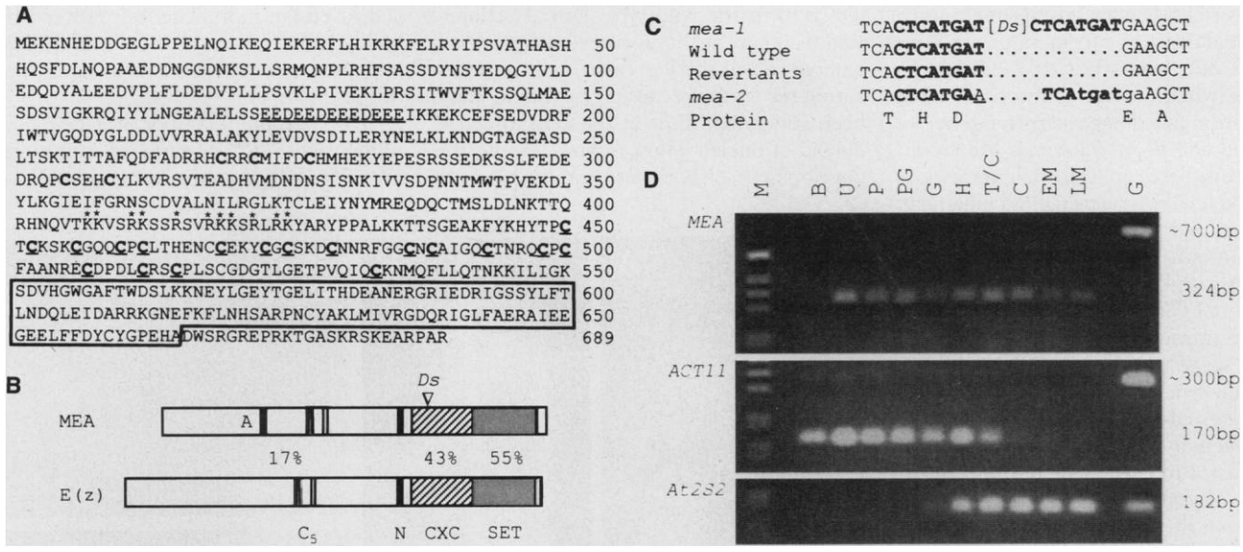

Fig. 2. Sequence analysis and expression profile of *MEA*. (**A**) Deduced amino acid sequence of *MEA* (*34*). An acidic region similar to that in the *trx* protein is underlined. The five cysteines that are conserved in *E(z)* homologs are boldface, and the 18 cysteine residues of the CXC domain are boldface and underlined. Basic residues of a putative bipartite nuclear localization signal are indicated by asterisks above the symbol. The 115–amino acid SET domain is boxed. (**B**) Schematic alignment of *MEA* and *E(z)* shows the relative position and amino acid identity of the SET and CXC domains, the putative nuclear localization signals (N), the five conserved cysteines (C_5), and the acidic domain (A). (**C**) DNA sequences flanking the *mea-1 Ds* insertion and derivative alleles. The 8-bp target site duplication is indicated by boldface. All revertants analyzed showed the wild-type sequence. In the stable *mea-2* excision allele, a 7-bp footprint remains; an additional base is altered (underlined). The *mea-2* footprint introduces two stop codons (lower case). (**D**) RT-PCR analysis of *MEA* during flower and seed development. The three panels show amplification of *MEA*, and actin-11 (*ACT11*) and the seed storage protein *At2S2* as controls for cDNA synthesis (*33*). RNA was isolated from floral buds (B), unpollinated carpels (U), pollinated carpels (P), and siliques containing embryos at the preglobular (PG), globular (G), heart (H), torpedo to early cotyledonary (T/C), cotyledonary (C), early (EM), and late maturation (LM) stages. (M) indicates the marker lane and (G) genomic DNA as a control.

ground, which produces diploid gametophytes carrying either none, one, or two *mea-1* alleles (*6*). Because tetraploids carrying one (simplex) or two (duplex) mutant alleles could have been recovered, we considered models for both possibilities with *mea-1* as either recessive or dominant (Table 2). The observed inheritance of seed abortion and kanamycin resistance is consistent with a simplex recessive model ($X^2 < \chi^2_{0.05[1]} = 3.84$). The recessive nature of *mea-1* is confirmed by the high transmission frequency of kanamycin resistance (247/331 = 75%). If *mea-1* was dominant, it would be exclusively transmitted through pollen at a frequency of about 47% in a simplex tetraploid (*7*). These results suggest that *mea* is a loss-of-function mutation. Thus, the wild-type function of *MEA* is to restrict cell proliferation during embryogenesis.

We cloned and characterized the *MEA* gene as *mea-1* was tagged with derivatives of the maize *Ac/Ds* transposon system (*8*): *mea-1* and the *Ds* element cosegregated without detectable recombination. This mutation was unstable in the presence of *Ac* transposase, and large revertant sectors could be identified in plants heterozygous for both *mea-1* and *Ac*. Using genomic fragments flanking the *Ds* element, we identified and sequenced a *MEA* cDNA (Fig. 2A) (*9*). The *MEA* gene is similar to *Enhancer of zeste* [*E(z)*], a *Drosophila melanogaster* protein involved in the regulation of homeotic genes. The highest similarity between the two proteins (55% amino acid identity) is found at the COOH-terminus (Fig. 2B), in the SET domain, which was named after the three founding members of the family in *Drosophila*—*Suppressor of variegation 3-9* [*Su(var)3-9*], *E(z)*, and *trithorax* (*trx*) (*10*, *11*). Although the function of the SET domain is unknown, members of this family are thought to regulate gene expression by associating with chromatin and controlling access of transcription factors (*12*). As members of the *Polycomb* and *trithorax* group, SET domain proteins regulate homeotic gene expression (*13*). Many show parent-of-origin–specific effects and regulate cell proliferation (*11*, *14*). For instance, the human homologs *All-1/Hrx* and *Enx-1* are involved in the control of lymphocyte proliferation (*15*), and the *Caenorhabditis elegans* homolog MES-2 supports survival of the germ line (*16*). The plant *E(z)* homolog *CURLY LEAF* (*CLF*) regulates expression of floral homeotic genes (*17*). *MEA* shares 43% identity with *E(z)* in the CXC domain, a cysteine-rich region NH_2-terminal to the SET domain (Fig. 2B). The CXC domain and five additional highly conserved cysteine residues (Fig. 2B) are unique to *E(z)* and its vertebrate and plant homologs (*17*). Although the function of these regions is unknown, they are required for *E(z)* activity (*18*). The similarity to SET domain proteins suggests that *MEA* con-

Table 2. Segregation of embryo lethality and kanamycin resistance in a 4n *mea* line. The tetraploid nature of this plant was confirmed at the cytogenetic level (*35*). Dry siliques were opened and their seeds classified as normal or aborted seeds displaying the *mea* phenotype. The progeny of this plant was tested for sensitivity (Kan^S) or resistance to kanamycin (Kan^R) linked to *mea-1*. Expected values of the two phenotypes scored are given for four different models [(1) to (4)]. For the calculation of expected progeny classes, a spontaneous embryo abortion rate of 1.5%, as determined for the parental tetraploid, was included. The coefficient of double reduction was taken as $c = 0.1$ (*29*).

Observed/expected	Aborted	Normal	X^2	Kan^R	Kan^S	X^2
Observed	17	182	–	247	84	–
(1) Simplex, *mea* recessive	15	184	0.29	237	94	1.48
(2) Duplex, *mea* recessive	48	151	26.4	314	17	278.4
(3) Simplex, *mea* dominant	98	101	131.9	155	176	102.7
(4) Duplex, *mea* dominant	161	38	674.5	265	66	6.1

trols cell proliferation by regulating gene expression through modulation of higher-order chromatin structure.

To confirm that the isolated gene corresponds to the *mea* mutation, we sequenced the region spanning the insertion site in three independently recovered revertants (*19*). The *Ds* element in *mea-1* inserted NH_2-terminal to residues of the SET domain that are invariant among the *E(z)* homologs. *Ds* excisions usually create characteristic footprints, and phenotypic revertants should restore the open reading frame of the disrupted gene. In all three revertants, the sequence was that of the wild type (Fig. 2C), indicating a strong sequence constraint on this region of the SET domain. In the phenotypically mutant excision allele *mea-2*, a 7–base pair (bp) footprint remains, introducing two stop codons (Fig. 2C).

We analyzed the expression profile of the *MEA* transcript using reverse transcription–polymerase chain reaction (RT-PCR) (*20*) on floral tissues and developing siliques (Fig. 2D). *MEA* is not expressed at early stages of flower development during early megagametogenesis. *MEA* expression is first detectable in unpollinated siliques that contain maturing gametophytes indicating maternal expression. The transcript remains detectable throughout the morphogenetic phase of embryogenesis and starts to disappear during seed maturation. Thus, *MEA* is either an unusually stable mRNA that is maternally deposited in egg or central cell, or both, and persists for 2 weeks throughout seed development or *MEA* is expressed both maternally and zygotically. *MEA* expression after fertilization may be regulated by genomic imprinting, because paternally provided copies cannot rescue embryo lethality.

The regulation of cell proliferation and growth during seed development by *MEA* is under maternal control. Haig and Westoby proposed that parent-of-origin–specific effects evolved as a consequence of an intragenomic conflict over the allocation of nutrients from the mother to its offspring (*21*). Although their theory is usually discussed with respect to imprinting, it is equally applicable to other postmeiotically established differences such as a maternal effect of cytoplasmic nature. The intragenomic conflict theory predicts that paternally expressed genes would tend to promote the growth of the embryo and maternally expressed genes would tend to reduce it. Supporting evidence has been provided by studies on imprinted genes in mice and humans (*22*) and from the manipulation of entire genomes in flowering plants (*23*). Our observations on the *mea* mutant phenotype suggest that similar molecular mechanisms operate in animals and plants to control cell proliferation and to mediate parent-of-origin–specific effects.

REFERENCES AND NOTES

1. Embryos and endosperm inheriting the mutant *mea* allele from the female gametophyte are referred to as *mea* embryos and *mea* endosperm.
2. Euripides (431 B.C.), *Medea*. Medea kills her two children in revenge for Jason's infidelity.
3. L. A. Castle *et al.*, *Mol. Gen. Genet.* **241**, 504 (1993); N. Ohad *et al.*, *Proc. Natl. Acad. Sci. U.S.A.* **93**, 5319 (1996); A. M. Chaudhury *et al.*, *ibid.* **94**, 4223 (1997).
4. S. Ray, T. Golden, A. Ray, *Dev. Biol.* **180**, 365 (1996); L. Colombo *et al.*, *Plant Cell* **9**, 703 (1997).
5. For whole-mount specimens, siliques were fixed in 3:1 ethanol:acetic acid for 2 hours and cleared in Hoyer's medium (*24*). For sectioning, siliques were fixed in 3% glutaraldehyde for 2 hours, rinsed in 50 mM cacodylate buffer, and postfixed in 2% OsO_4. After serial dehydration in ethanol, specimens were embedded in Spurr's media (*25*). Seeds were observed, using bright-field and differential interference contrast optics.
6. *mea* was crossed to a tetraploid, and triploid progeny carrying *mea* were allowed to self-fertilize. Triploid plants produce few seeds, most of which are small [aneuploid; (*26*)], whereas rare tetraploid seeds are larger than diploid wild-type seeds. Large seeds were selected, and tetraploid plants were identified on the basis of morphology (*27*), reduced seed set, and altered segregation pattern of *mea* seeds. Their tetraploid nature was verified by chromosome counts of 4′,6′-diamidino-2-phenylindole–stained root tip preparations as described (*28*).
7. Transmission was calculated by taking the coefficient of double reduction (the frequency at which the alleles of two sister chromatids are recovered in the same gamete) $c = 0.1$ as previously estimated for this chromosomal region.
8. V. Sundaresan *et al.*, *Genes Dev.* **9**, 1797 (1995); P. S. Springer, W. R. McCombie, V. Sundaresan, R. Martienssen, *Science* **268**, 877 (1995).
9. Genomic DNA flanking the *mea-1 Ds* insertion was isolated by thermal asymmetric interlaced PCR (TAIL-PCR) (*30*): Three nested primers for the 5′ and 3′ end of *Ds* were used in consecutive PCR reactions in combination with either the AD1 or AD2 primer (*30*). Conditions were as in (*30*), with minor modifications: The primary PCR reaction was incubated at 95°C for 2 min before initiating the high-stringency cycles. We performed 15 supercycles in the secondary reaction and 25 low-stringency cycles in the tertiary reaction. Nested *Ds* primers were: Ds5-1 (5′-CCGTTTACCGTTTTGTATATCCCG-3′), Ds5-2 (5′-CGTTCCGTTTTCGTTTTTTTACC-3′), Ds5-3 (5′-GGTCGGTACGGGAATTCTCCC-3′), Ds3-1 (5′-CGATTACCGTATTTATCCCGTTCG-3′), Ds3-2 (5′-CCGGTATATCCCGTTTTCG-3′), and Ds3-3 (5′-GTTACCGACCGTTTTCATCC-3′). PCR products were subcloned into the pTAdvantage vector (Clontech). We screened 8×10^5 phages from a flower cDNA library (*31*), using a 3′ TAIL-PCR subclone (mah17) as a probe. A single cDNA phage was isolated. The plasmid was excised using the ExAssist helper phage and sequenced. The cDNA contained a polyadenylated tail, but was not full length. The 5′ end was isolated by 5′ RACE PCR: 1 mg of total RNA from young siliques was reverse transcribed using 2.5 pmol of meaAS3 (5′-CCAGCAGTTCCATCATTC-3′) in a 20-μl reaction containing 1× PCR buffer (Gibco-BRL), 2.5 mM $MgCl_2$, 0.5 mM each deoxynucleotide triphosphate (dNTP), 10 mM dithiothreitol, and 200 units of Superscript reverse transcriptase (Gibco-BRL) by incubating at 42°C for 1 hour. After heat inactivation at 70°C for 20 min, the sample was treated with 2 units of ribonuclease H (RNAse H) (Gibco-BRL) at 37°C for 30 min. The cDNA was purified with the PCR Purification kit (Perkin-Elmer/Cetus). We treated one-fifth of the sample with 15 units of terminal deoxynucleotidyl transferase (Gibco-BRL) in 10 mM tris (pH 8.4), 25 mM KCl, 1.5 mM $MgCl_2$, and 0.2 mM deoxycytidine triphosphate at 37°C for 10 min, followed by heat inactivation at 65°C. The first round of PCR was performed in 1× PCR buffer (Perkin-Elmer), 2 mM $MgCl_2$, 0.2 mM each dNTP, 1 unit of Taq polymerase (Perkin-Elmer/Cetus), and 20 pmol of each primer—5RACE Abridged Adapter Primer (5RACEAAP, Gibco-BRL) and meaAS4 (5′-GTCCGAAACATCCACTTCG-3′)—for 35 cycles at an annealing temperature of 55°C. We used one-twentieth of the product in the second round of PCR performed under the same conditions but with the primers Abridged Universal Adapter Primer (AUAP, Gibco-BRL) and meaAS5 (5′-CGACCAGATCATCCAAACCATAG-3′). The PCR products were ligated into the pTAdvantage vector (Clontech); four subclones were sequenced to derive a composite cDNA sequence.
10. B. Tschiersch *et al.*, *EMBO J.* **13**, 3822 (1994); A. M. Mazo, D.-H. Huang, B. A. Mozer, I. B. David, *Proc. Natl. Acad. Sci. U.S.A.* **87**, 2112 (1990).
11. R. S. Jones and W. M. Gelbart, *Mol. Cell. Biol.* **13**, 6357 (1993).
12. V. Orlando and R. Paro, *Curr. Opin. Genet. Dev.* **5**, 174 (1995); V. Pirrotta, *ibid.* **7**, 249 (1997).
13. J. Simon, *Curr. Opin. Cell Biol.* **7**, 376 (1995); M. J. Alkema *et al.*, *Nature* **374**, 724 (1995); B. D. Yu *et al.*, *ibid.* **378**, 595 (1995).
14. M. Gatti and B. S. Baker, *Genes Dev.* **3**, 438 (1989); M. D. Phillips and A. Shearn, *Genetics* **125**, 91 (1990).
15. D. C. Tkachuk, S. Kohler, M. L. Cleary, *Cell* **71**, 869 (1992); Y. Gu *et al.*, *ibid.*, p. 701; O. Hobert, B. Jallal, A. Ullrich, *Mol. Cell. Biol.* **16**, 3066 (1996).
16. E. E. Capowski, P. Martin, C. Garvin, S. Strome, *Genetics* **129**, 1061 (1991); R. Holdeman, S. Nehrt, S. Strome, personal communication.
17. J. Goodrich *et al.*, *Nature* **386**, 44 (1997).
18. E. A. Carrington and R. S. Jones, *Development* **122**, 4073 (1996).
19. Genomic DNA from Landsberg *erecta* wild-type plants, *mea-1* and *mea-2* heterozygotes, and seedlings derived from three independent revertant sectors was isolated (*32*). The junction fragments were amplified by PCR in 1× PCR buffer (Perkin-Elmer) containing 2 mM $MgCl_2$, 0.2 mM each dNTP, 1 unit of Taq DNA polymerase (Perkin-Elmer/Cetus), and 40 pmol of each specific primer for 40 cycles at an annealing temperature of 55°C. The primers were mea5-3 (5′-CGTAGCAGTTAGGTCTTGC-3′) and mea3-1 (5′-CGTCGACCCGTCAGGACTCTC-3′). For *mea-1* DNA, mea5-3 and mea3-1 were used in combination with primers Ds5-2 and Ds3-2 (*9*), respectively. The PCR products were ligated into the pTAdvantage vector (Clontech), and four to five subclones were sequenced for each derivative allele.
20. For RNA preparation, tissue from wild-type Landsberg *erecta* plants was harvested in liquid nitrogen. RNA from buds, unpollinated and pollinated carpels, and young siliques was prepared using the Trizol LS reagent (Gibco-BRL). RNA from tissues high in starch content was prepared using the Qiagen RNeasy kit (Qiagen). For accurate sampling, the stage to which embryogenesis had progressed was determined for each silique. For RT-PCR, 5 mg of total RNA was treated with 5 units of RNAse-free deoxyribonuclease in 1× PCR buffer (Gibco-BRL) containing 2.5 mM $MgCl_2$. After heat inactivation at 80°C for 5 min, the samples were extracted with phenol–chloroform–isoamyl alcohol (25:24:1) and then were precipitated with ethanol. The RNA was reverse transcribed using 5 pmol of random hexamers (Pharmacia Biotech) (*9*). We used one-fifth of the cDNA samples for PCR amplification of *MEA*; one-tenth of the samples was used to amplify *ACT11* and *At2S2* (*33*). PCR was performed in 1× PCR buffer (Perkin-Elmer) containing 2 mM $MgCl_2$, 0.2 mM each dNTP, 1 unit of Taq DNA polymerase (Perkin-Elmer/Cetus), and 20 pmol of each gene-specific primer for 30 cycles at an annealing temperature of 55°C. The primers used for amplification were: meaS4 (5′-GCAGGACTATGGTTTGGATG-3′) and meaAS6 (5′-CACCTTGAGGTAACAATGCTC-3′) for *MEA*, Act11F (5′-AACTTTC-

AACACTCCTGCCATG-3′) and Act11R (5′-CTGCAAGGTCCAAACGCAGA-3′) for *ACT11*, and At2S2F (5′-GAGCCAGTTTGTGTTTGC-3′) and At2S2R (5′-TAAGGAGGGAAGAAAGGG-3′) for *At2S2*.
21. D. Haig and M. Westoby, *Am. Nat.* **134**, 147 (1989).
22. D. Haig and C. Graham, *Cell* **64**, 1045 (1991); R. Jaenisch, *Trends Genet.* **13**, 323 (1997); W. Reik and E. R. Maher, *ibid.*, p. 330.
23. B.-Y. Lin, *Genetics* **100**, 475 (1982); J. Kermicle and M. Alleman, *Development (Suppl.)* **1**, 9 (1990); D. Haig and M. Westoby, *Philos. Trans. R. Soc. London Ser. B* **333**, 1 (1991).
24. T. Berleth and G. Jürgens, *Development* **118**, 575 (1993).
25. A. R. Spurr, *J. Ultrastruct. Res.* **26**, 31 (1969).
26. G. Röbbelen and F. J. Kribben, *Arabidopsis Inf. Serv.* **3**, 16 (1966).
27. J. Bouharmont and F. Macé, *Can. J. Genet. Cytol.* **14**, 257 (1972).
28. J. Maluszynska and J. S. Heslop-Harrison, *Ann. Bot. (London)* **71**, 479 (1993).
29. J. H. van der Veen and H. Blankenstijn–de Vries, *Arabidopsis Inf. Serv.* **10**, 11 (1973).
30. J.-G. Liu *et al.*, *Plant J.* **8**, 457 (1995).
31. D. Weigel *et al.*, *Cell* **69**, 843 (1992).
32. K. Edwards, C. Johnstone, C. Thompson, *Nucleic Acids Res.* **19**, 1349 (1991).
33. J. M. McDowell *et al.*, *Genetics* **142**, 587 (1996); P. Guerche *et al.*, *Plant Cell* **2**, 469 (1990).
34. Single-letter abbreviations for the amino acid residues are as follows: A, Ala; C, Cys; D, Asp; E, Glu; F, Phe; G, Gly; H, His; I, Ile; K, Lys; L, Leu; M, Met; N, Asn; P, Pro; Q, Gln; R, Arg; S, Ser; T, Thr; V, Val; W, Trp; and Y, Tyr.
35. J.-P. Vielle-Calzada and U. Grossniklaus, data not shown.
36. We thank J. Moore for help with the mutagenesis, M. Koornneef for providing the parental tetraploid line, W. Herr, R. Martienssen, and B. Stillman for comments on the manuscript, and the Hernandez, Hengartner, and Stillman laboratories for space on sequencing gels. Special thanks go to V. Sundaresan and R. Martienssen for providing us access to their insertional mutagenesis system before publication and to S. Strome for allowing us to cite unpublished data. Supported by the Cold Spring Harbor Laboratory President's Council, the Robertson Research Foundation, and fellowships from the European Molecular Biology Organization, the Human Frontier Science Program, and the Janggen-Poehn Foundation to U.G.

18 September 1997; accepted 9 February 1998

Cathepsin L: Critical Role in Ii Degradation and CD4 T Cell Selection in the Thymus

Terry Nakagawa,* Wera Roth,* Phillip Wong, Andrew Nelson, Andrew Farr, Jan Deussing, Jose A. Villadangos, Hidde Ploegh, Christoph Peters, Alexander Y. Rudensky†

Degradation of invariant chain (Ii) is a critical step in major histocompatibility complex class II–restricted antigen presentation. Cathepsin L was found to be necessary for Ii degradation in cortical thymic epithelial cells (cTECs), but not in bone marrow (BM)–derived antigen-presenting cells (APCs). Consequently, positive selection of $CD4^+$ T cells was reduced. Because different cysteine proteinases are responsible for specific Ii degradation steps in cTECs and BM-derived APCs, the proteolytic environment in cells mediating positive and negative selection may be distinct. The identification of a protease involved in class II presentation in a tissue-specific manner suggests a potential means of manipulating $CD4^+$ T cell responsiveness in vivo.

Major histocompatibility complex (MHC) class II molecules are assembled with the assistance of Ii in the endoplasmic reticulum (ER) and transported to an endocytic compartment where Ii undergoes rapid degradation by lysosomal proteinases (*1*). Peptides derived from amino acids 81 to 104 of Ii are termed CLIP (class II–associated Ii peptides), and remain bound in the class II peptide binding groove, until removed by the chaperone molecule H-2M (*1*). This allows peptides derived from the proteolytic degradation of foreign and self proteins (*2*) to then bind class II molecules and appear on the cell surface. Self peptide–class II complexes expressed on cTECs positively select maturing $CD4^+$ T cells, whereas those expressed by BM-derived APCs mediate negative selection (*3*).

Cathepsins are lysosomal endoproteinases that have been implicated in the MHC class II processing pathway by in vitro studies using purified enzymes or cathepsin inhibitors (*4*). Because of the apparent redundancy of these enzymes and the inherent difficulty of mimicking the complex proteolytic environment of endocytic compartments, the specific role of cathepsins in the class II presentation pathway in vivo remains unclear. Generation of cathepsin-deficient mice (*5*, *6*) provided a direct experimental approach toward the elucidation of their specific functions and targets.

Cathepsin L (CTSL)–deficient mice have periodic shedding of fur and abnormal skin morphology, which recapitulate the spontaneous mouse mutation *furless* (*6*). To assess the role of CTSL in the class II presentation pathway, we examined splenic APCs from $ctsl^{-/-}$ and littermate control mice (Fig. 1A). Flow cytometric analysis of these cells stained with monoclonal antibodies (mAbs) specific for several independent I-A^b epitopes, and for I-A^b bound to CLIP (*7*) and non-CLIP peptides (*8*), did not reveal any effects of the CTSL mutation on class II expression. Similarly, class II expression was not altered in splenic dendritic cells (sDCs) and thioglycollate-activated, interferon-γ–induced peritoneal macrophages (pMph) (*9*). In addition, splenocytes, sDCs and peritoneal Mph from $ctsl^{-/-}$, $ctsl^{+/-}$, and wild-type (WT) mice did not reveal significant differences in the amounts of Ii or SDS-stable and SDS-unstable I-A^b dimers (*9*). No differences were found in presentation by $ctsl^{-/-}$ and littermate control splenocytes or peritoneal macrophages of a broad range of foreign and self antigens, including hen egg lysozyme, ribonuclease A (RNase A), *Trypanosoma cruzi* SA85 major surface antigen, heat-killed *Chlamydia trachomatis*, immunoglobulin M (IgM), β_2-microglobulin (β_2-M), H-2M, and actin (Fig. 1B) (*9*). Thus, class II expression in peripheral APCs and their ability to present self and foreign antigens were not impaired in $ctsl^{-/-}$ mice. This finding, in conjunction with the observation of normal class II presentation in cathepsin B null ($ctsb^{-/-}$) mice (*9*), implied that another cysteine proteinase, perhaps cathepsin S (CTSS) (*10*), must be involved in class II processing in peripheral APCs.

To determine whether the CTSL deficiency affects $CD4^+$ T cell selection, we next analyzed thymocytes and splenocytes from $ctsl^{-/-}$, $ctsl^{+/-}$, and WT mice for CD4, CD8, and T cell antigen receptor (TCR) expression. Although the total cellularity of the lymphoid organs in all these mice was comparable, $ctsl^{-/-}$ mice had reduced numbers of $CD4^+$ T cells in the thymus and periphery (~60 to 80% reduction) (Fig. 2A). Consequently, $CD8^+$ T cells were relatively increased. In contrast, T cell subsets were normal in $ctsl^{+/-}$ littermates and in cathepsin B ($ctsb^{-/-}$) and D ($ctsd^{-/-}$) null mice (Fig. 3) (*9*). Purified $CD4^+$ T cells isolated from immunized $ctsl^{-/-}$ mice were

T. Nakagawa, P. Wong, A. Y. Rudensky, Howard Hughes Medical Institute and Department of Immunology, University of Washington School of Medicine, Seattle, WA 98195, USA.
W. Roth, J. Deussing, C. Peters, Medizinische Molekularbiologie, Abteilung Heamatologie-Onkologie, Klinikum der Albert-Ludwigs-Universitat Freiburg, 79106 Freiburg, Germany.
A. Nelson and A. Farr, Department of Biological Structure and Department of Immunology, University of Washington School of Medicine, Seattle, WA 98195, USA.
J. A. Villadangos and H. Ploegh, Department of Pathology, Harvard Medical School, Boston, MA 02115, USA.

*These authors contributed equally to this work.
†To whom correspondence should be addressed: E-mail: sasha@nucleus.immunol.washington.edu